

Determining granular behavioural zones in rotating tumblers

François Guillard^{1,*}, Paul Shelley^{2,**}, and Itai Einav^{1,***}

¹School of Civil Engineering, The University of Sydney, NSW 2006, Australia.

²Molycop, 18-22 Jackson St, Bassendean, WA 6054, Australia.

Abstract. The wide range of behaviour exhibited by granular flows has made them challenging to handle practically. For example, rotary mills used for grinding mining materials operate in the cataracting regime, which combines the whole range of flowing conditions for granular materials, including solid body motion, dense flow, and gaseous collisional regime. A good understanding of the material behaviour in such processes is crucial to optimise industrial operating conditions; however, this is rendered difficult by the large scales of the operations and the complexity of probing the charge inside the mills. In this paper, we present a method allowing for both comprehensive and manageable understanding of the local granular material behaviour, applicable to a wide variety of situations. Inspired by the example case of rotary mills, we perform discrete element numerical simulations of a rotating tumbler with lifters and extract the local fields of interest, such as strains, pressures, and density, through standard coarse-graining methods. Those smooth fields are then appropriately non-dimensionalised, and used as input for a clustering algorithm. The clustering allows pinpointing of distinct zones of behaviour in the tumbler. Crucially, those zones have well-identified physical properties, and are relevant to the whole range of rotation rates. These zones allow us to numerically study how the flow is affected by changes in operating conditions, similar field measurements in industry operating conditions are difficult to acquire due to the opacity of the mill and the harsh environment. We complement the numerical analysis by in-situ measurements in a laboratory scale three-dimensional rotating tumbler. We use recent technological advances in embedded sensors and X-ray dynamic radiography reconstruction to provide new insights into the behaviour of rotary mills, measuring particle trajectories and accelerations directly inside the mill. The analysis and experimental methods presented provide new tools and insights to analyse complex granular flows. They apply to the full range of granular regimes, and can be extended to a broad range of geometries and processes.

1 Introduction

Rotating tumblers have been extensively studied in the field of granular materials, because of the simplicity of their geometry combined with the broad range of regimes of behaviour they exhibit [1, 2]. Crucially, they are also part of many industrial processes, from chemical reactors for pharmaceutical manufacturing, to ore crushing and mineral extraction in Semi-Autogenous Grinding mills in the mining industry. In those contexts, a good understanding of the rotating tumbler system is important to ensure the quality of the processed product while maintaining the efficiency of the system.

However, industrially, the information available on the system, especially for large scale mills, is limited. Some external information such as power input or force sensors on the mill walls may provide useful data [3]. In addition, instrumented balls have been developed to be added to the grinding media, providing spot measurements of acceleration inside the mill, but unfortunately without the knowledge of the location where these measurements are taken given that the material is in rapid motion [4].

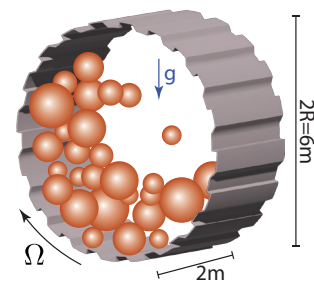


Figure 1. Sketch of the simulations performed.

Numerically, simulations of the entire system remain challenging and are often limited to overall population balance [5], although more advanced and accurate numerical tools may allow for a more precise description of the evolution of the material over time [6]. Discrete Element Modelling (DEM), on the other hand, is quickly limited by the amount of material that can be simulated in a reasonable time, and provide results that are difficult to handle and use without further processing. Discrete information from each grain is usually too noisy to be useful, and the spatially averaged fields resulting from coarse-graining

*e-mail: francois.guillard@sydney.edu.au

**e-mail: paul.shelley@molycop.com

***e-mail: itai.einav@sydney.edu.au

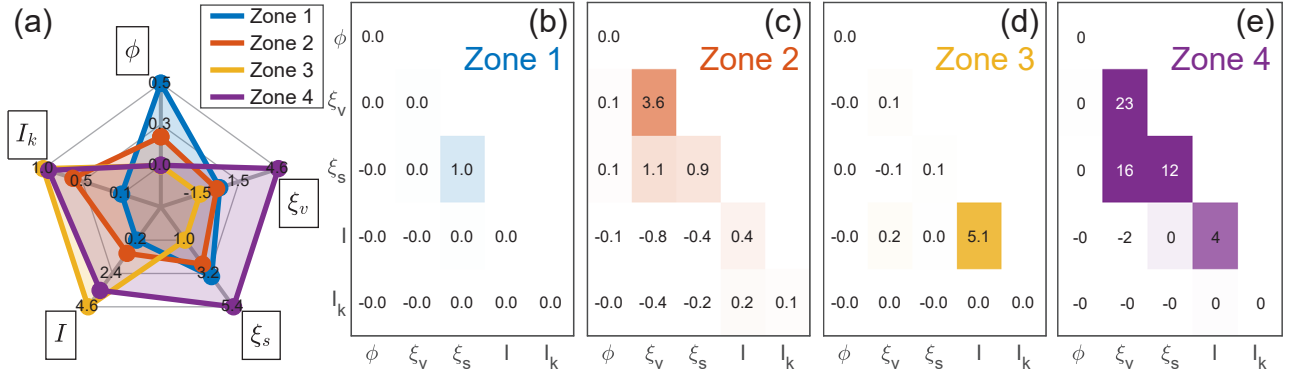


Figure 2. Properties of the identified clusters. (a) Average value μ_n for all zones, and (b-e) covariance matrices \mathbf{S}_n for zones 1-4, respectively. Note that \mathbf{S} is symmetric so only the bottom half of the matrix is displayed. Diagonal values are the variance of the corresponding variable.

may be difficult to handle altogether and effectively provide too detailed a picture of the system to give meaningful industrial information for decision-making.

In this paper, we propose a method to rationalise DEM results into a set of distinct behavioural zones, that objectively and physically distinguishes regimes of material flow, linked to well-defined physical properties. This will be accomplished on the example of a tumbler rotating tumbler simulated using Liggghts [7]. The data from the simulations will then be coarse-grained, before being non-dimensionalised and processed through a clustering algorithm, providing information on the flow behaviour for various rotational speed. Finally, we will discuss how such information can be validated experimentally, and the opportunities provided by internal measurement sensors and external x-ray imaging.

2 Behavioural zone identification

2.1 Description of the simulations

We simulate a tumbler of radius $R = 3$ m and depth 2 m rotating along its horizontal axis at an angular speed Ω , with lifters on the walls to ensure proper mobilisation of the grains (Fig. 1). The material is composed of 45,000 particles of diameter ranging from 1 to 10 cm ($d_{50} = 5$ cm) and density $\rho_g = 2500$ kg.m⁻³, interacting through inelastic Hertzian contact (Young's module 500 MPa, Poisson ratio 0.3, restitution coefficient 0.6) with friction (friction coefficient 0.5) [8]. More details about the simulations are available in [9]. Once a steady state of rotation is established for the charge, we perform coarse-graining using a Lucy windowing function of width 0.4 m [9–11].

2.2 Non-dimensionalisation

The usual kinematic fields of interest are obtained from coarse-graining, namely the density field ρ , pressure P , itself the sum of the contact and kinetic pressure P_k , as well as the velocity field from which the volumetric $\dot{\epsilon}_v$ and shear strain rate $\dot{\epsilon}_s$ invariants are extracted. In this state, those fields cannot be compared and used for clustering in

an appropriate way, since they carry physical units. This is solved by non-dimensionalising the variable with the characteristic scales of the system. Following previous approaches, it is therefore natural to define the following five non-dimensional variables:

$$\phi = \rho/\rho_g; \quad \xi_v = \dot{\epsilon}_v/\Omega; \quad I = d_{50}\dot{\epsilon}_s(\rho_g/P)^{1/2}; \quad (1)$$

$$\xi_s = \dot{\epsilon}_s/\Omega; \quad I_k = P_k/P.$$

In this set of equations, ϕ is the volume fraction, ξ_v and ξ_s represent scaled strain rates based on the strain rate Ω imposed by the rotation of the mill, I follows the standard inertial number definition [12, 13] typically used to characterise the regime of behaviour of dense flows, and I_k is the kinetic number, characterising the transition between dense and gaseous regimes of granular systems, which appears relevant for granular models [14, 15].

2.3 Clustering

The five non-dimensional numbers above are measured at every coarse-graining point in the system. It is therefore possible to identify if different points have similar behaviours on the basis of the values of these fields. This is done using a Gaussian Mixture Model clustering algorithm, which has the advantage of providing direct physical meaning to the clusters obtained [16]. The general idea is that every data point i corresponds to a point in the five-dimensional space of non-dimensional variables $\mathbf{x}^i = (\phi^i, \xi_v^i, \xi_s^i, I^i, I_k^i)$. Then, the number N of clusters that should be identified is chosen, and N Gaussian multivariate probability distributions are then best fitted to the dataset, such that the probability of an observation \mathbf{x} is given by [16]:

$$p(\mathbf{x}) = \sum_{n=0}^N w_n \frac{\exp(-(\mathbf{x} - \boldsymbol{\mu}_n)^T \mathbf{S}_n (\mathbf{x} - \boldsymbol{\mu}_n)/2)}{(2\pi)^{D/2} |\mathbf{S}_n|^{1/2}} \quad (2)$$

with $\boldsymbol{\mu}_n$ and \mathbf{S}_n the vector of means and covariance matrix for distribution n , respectively. D is the dimension of the variable space, equal to 5 here. Once the distributions have been identified, the corresponding weights w_n of each data

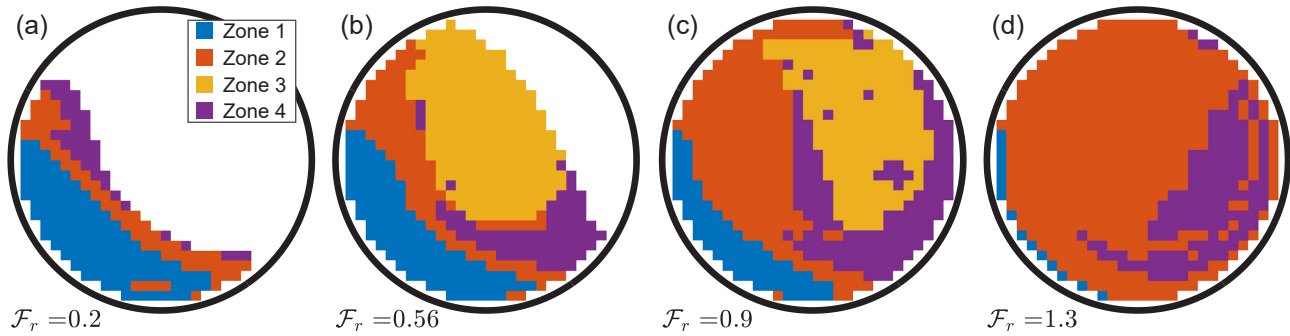


Figure 3. Identified zones for tumblers rotating with different Froude numbers.

point are calculated, and the data is assigned to the cluster with highest weight.

There are two important points of note here. Firstly, the probability distribution identification and the data allocation can be performed on the same dataset, or on different datasets. In the latter case, this means that clusters can be identified in a particular simulation and applied in any other simulations while retaining the same physical meaning. Secondly, the number of clusters N needs to be chosen *a priori*. While there are methods to relax this requirement, here we are choosing $N = 4$ for simplicity. The effect of the number of clusters chosen can be seen in [9].

3 Results

Following the previous procedure, we apply the clustering with $N = 4$ clusters on a rotating tumbler simulation with a Froude number $\mathcal{F}_r = R\Omega^2/g = 0.56$, corresponding to the cataracting regime. This was chosen to cover all regimes of granular behaviour within a single simulation. As indicated, the identified clusters have a clear meaning in terms of the non-dimensional variables in Eq. 1, and Fig. 2a shows their average value μ_n and covariance matrices ζ_n . Additionally, Fig. 3b shows the cluster to which each point in space was allocated. As it is evident that zones in space tend to correspond to specific clusters, we will use the two terms interchangeably from now on. Note that only a central slice through the tumbler is represented as three-dimensional effects have been observed to be minimal.

It is clear that each zone is well identified by their physical properties. Zone 1 corresponds to a denser region with limited flow. Zone 2 shows greater motion with higher I and I_k and a lowering of the volume fraction as the material gets lifted in the tumbler, supported by the large variance of ξ_v observed in that zone. Zone 3 essentially corresponds to the free fall of the grains, with low density and high I , emerging from the drop in contact stresses. Finally, zone 4 corresponds to the impact zone, and the agitation in that zone results in large values of the variances and covariances between the non-dimensional variables.

The identified zones are consistent with previous observations [17, 18], and have the benefit of providing an objective way of classifying the flow with clear physical

meaning for the zones. The clusters identified for the simulations at $\mathcal{F}_r = 0.56$ can now be applied to other simulations, as shown in Fig. 3. It is clear that the zones identified remain relevant for a broad range of Froude number. At low Froude (Fig. 3a), zones 3 and 4 remain confined to the very top layer of the avalanching flow, while zone 2 identifies the dense flow layer and zone 1 the solid body rotation. At larger rotational velocities (Fig. 3c-d, $\mathcal{F}_r \sim 1$), zone 1 reduces and all but disappears, and all the grains are agitated in zones 2 and 4. Eventually, we would expect simulations at $\mathcal{F}_r \gg 1$ in the centrifugal regime to have a zone 1 layer only on the periphery of the tumbler.

4 Towards experimental validation

The framework highlighted above relies on the detailed knowledge of the local kinematic properties to perform the clustering analysis. While these data are straightforward to obtain in simulations, they are significantly more challenging to obtain experimentally or in the field. Conversely, numerical simulations are limited on the scale of problem they can tackle, and large numbers of grains or the presence of fluid can simply make them computationally unachievable.

Recent experimental advances have unlocked some of those limitations though. At laboratory scale, X-ray radiography allows probing the material and access to the density field [19] and velocity fields [20, 21] of flowing granular materials. In-situ measurements using instrumented particles are also possible, even at laboratory scale thanks to advances in electronic miniaturisation (Fig. 4a-b), and have been used at industrial scales as well.

Fig. 4c shows an example of such a method. An instrumented particle is measuring its own acceleration a and angular velocity ω *in-situ* in a tumbler rotating with $\mathcal{F}_r = 0.09$, while two x-ray source-detectors pairs are imaging the setup. This allows for the triangulation of the location of the particle. Fig. 4d shows the time signal of the angular location θ , and Fig. 4e displays the magnitude of a and ω on the same timescale. It is clear that the location of the instrumented particle is correlated with the acceleration it is recording, unlocking the ability to identify how the particle acceleration changes as the particle travels between different zones of the flow within the tumbler.

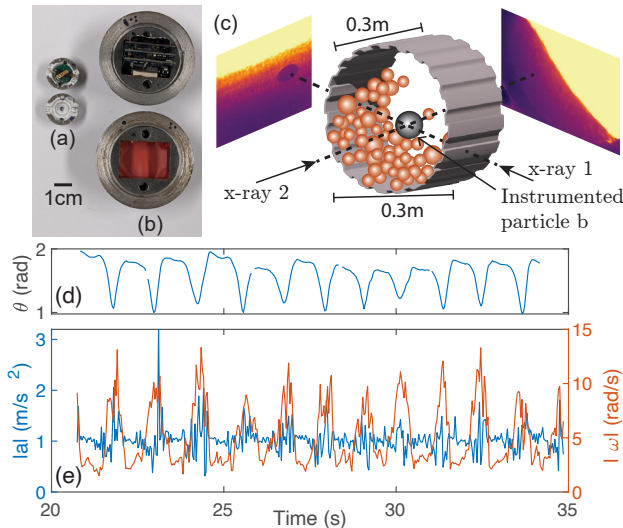


Figure 4. (a-b) Examples of instrumented particles. (c) Rotating tumbler with instrumented particle and double x-ray imaging for triangulation. (d) Angular location from x-ray measurement. (e) Acceleration and angular velocity from instrumented particle measurements.

5 Conclusion

In conclusion, we have developed a methodology that is able to identify distinct behavioural zones with well defined physical meaning in a granular flow. While the method was applied to rotating tumbler flows, it should be straightforward to apply it to other geometries, providing a clear pathway to obtain useful information on local flow properties. Eventually, this information can be coupled with measurements performed in-situ at laboratory or field scale to better understand the internal material flow conditions.

References

- [1] J. Rajchenbach, Flow in powders: From discrete avalanches to continuous regime, *Physical review letters* **65**, 2221 (1990).
- [2] I. Govender, Granular flows in rotating drums: A rheological perspective, *Minerals Engineering* **92**, 168 (2016). <https://doi.org/10.1016/j.mineng.2016.03.021>
- [3] J. Campbell, S. Spencer, D. Sutherland, T. Rowlands, K. Weller, P. Cleary, A. Hinde, Sag mill monitoring using surface vibrations, *Proceedings International autogenous and semiautogenous grinding technology pp.* 373–385 (2001).
- [4] S. Martins, W. Li, P. Radziszewski, S. Caron, M. Aguanno, M. Bakhos, E.L. Petch, Validating the instrumented ball outputs with simple trajectories, *Minerals Engineering* **21**, 782 (2008). [10.1016/j.mineng.2008.05.016](https://doi.org/10.1016/j.mineng.2008.05.016)
- [5] M. Bueno, T. Kojovic, M. Powell, F. Shi, Multi-component ag/sag mill model, *Minerals Engineering* **43**, 12 (2013).
- [6] M.S. Bisht, F. Guillard, P. Shelley, B. Marks, I. Einav, Heterarchical modelling of comminution for rotary mills: part I—particle crushing along streamlines, *Granular Matter* **26**, 88 (2024).
- [7] C. Kloss, C. Goniva, A. Hager, S. Amberger, S. Pirker, Models, algorithms and validation for opensource DEM and CFD–DEM, *Progress in Computational Fluid Dynamics, an International Journal* **12**, 140 (2012).
- [8] N.V. Brilliantov, F. Spahn, J.M. Hertzsch, T. Pöschel, Model for collisions in granular gases, *Physical review E* **53**, 5382 (1996).
- [9] F. Guillard, P. Shelley, I. Einav, Behavioural zone identification in rotary mills, *Minerals Engineering* **212**, 108711 (2024).
- [10] B.J. Glasser, I. Goldhirsch, Scale dependence, correlations, and fluctuations of stresses in rapid granular flows, *Physics of Fluids* **13**, 407 (2001). [10.1063/1.1338543](https://doi.org/10.1063/1.1338543)
- [11] T. Weinhart, R. Hartkamp, A.R. Thornton, S. Luding, Coarse-grained local and objective continuum description of three-dimensional granular flows down an inclined surface, *Physics of Fluids* **25**, 070605 (2013). [10.1063/1.4812809](https://doi.org/10.1063/1.4812809)
- [12] GDR MiDi, On dense granular flows, *The European Physical Journal E* **14**, 341 (2004).
- [13] P. Jop, Y. Forterre, O. Pouliquen, A constitutive law for dense granular flows, *Nature* **441**, 727 (2006). [10.1038/nature04801](https://doi.org/10.1038/nature04801)
- [14] E. Alaei, B. Marks, I. Einav, A hydrodynamic-plastic formulation for modelling sand using a minimal set of parameters, *Journal of the Mechanics and Physics of Solids* **151**, 104388 (2021). [10.1016/j.jmps.2021.104388](https://doi.org/10.1016/j.jmps.2021.104388)
- [15] D. Riley, I. Einav, F. Guillard, A constitutive model for porous media with recurring stress drops: From snow to foams and cereals, *International Journal of Solids and Structures* **262**, 112044 (2023).
- [16] D.A. Reynolds et al., Gaussian mixture models., *Encyclopedia of biometrics* **741** (2009).
- [17] K.S. Liddell, Ph.D. thesis, M. Sc. thesis, University of the Witwatersrand (1986)
- [18] V. Buchholtz, J.A. Freund, T. Pöschel, Molecular dynamics of comminution in ball mills, *The European Physical Journal B-Condensed Matter and Complex Systems* **16**, 169 (2000).
- [19] S. Méjean, F. Guillard, T. Faug, I. Einav, Length of standing jumps along granular flows down smooth inclines, *Physical Review Fluids* **5**, 034303 (2020).
- [20] F. Guillard, B. Marks, I. Einav, Dynamic x-ray radiography reveals particle size and shape orientation fields during granular flow, *Scientific reports* **7**, 8155 (2017).
- [21] J. Baker, F. Guillard, B. Marks, I. Einav, X-ray rheography uncovers planar granular flows despite non-planar walls, *Nature communications* **9**, 5119 (2018).